Published in final edited form as:
Exp Lung Res. 2012 October ; 38(8): 396–405. doi:10.3109/01902148.2012.715364.

Mechanostructural Adaptations Preceding Post-Pneumonectomy Lung Growth

Barry C. Gibney[1], **Jan P. Houdek**[2], **Kenji Chamoto**[1], **Grace S. Lee**[1], **Maximilian Ackermann**[2], **Miao Lin**[1], **Dinee Collings-Simpson**[1], **Moritz A. Konerding**[2], **Akira Tsuda**[3], and **Steven J. Mentzer**[1]

[1]Laboratory of Adaptive and Regenerative Biology, Brigham & Women's Hospital, Harvard, Medical School, Boston MA

[2]Institute of Functional and Clinical Anatomy, University Medical Center of the Johannes Gutenberg-University Mainz, Germany

[3]Molecular and Integrative Physiological Sciences, Harvard School of Public Health, Boston, MA

Abstract

In many species, pneumonectomy results in compensatory growth in the remaining lung. Although the late mechanical consequences of murine pneumonectomy are known, little is known about the anatomic adaptations and respiratory mechanics during compensatory lung growth. To investigate the structural and mechanical changes during compensatory growth, mice were studied for 21 days after left pneumonectomy using microCT and respiratory system impedance (FlexiVent). Anatomic changes after left pneumonectomy included minimal mediastinal shift or chestwall remodeling, but significant displacement of the heart and cardiac lobe. Mean displacement of the cardiac lobe centroid was 5.2±0.8mm. Lung impedance measurements were used to investigate the associated changes in respiratory mechanics. Quasi-static pressure-volume loops demonstrated progressive increase in volumes with decreased distensibility. Measures of quasi-static compliance and elastance were increased at all time points post pneumonectomy ($p < 0.01$). Oscillatory mechanics demonstrated a significant change in tissue impedance on the 3rd day after pneumonectomy. The input impedance on day 3 after pneumonectomy demonstrated a significant increase in tissue damping (5.8 versus 4.3 cmH_2O/ml) and elastance (36.7 versus 26.6 cmH_2O/ml) when compared to controls. At all points, hysteresivity was unchanged (0.17). We conclude that the timing and duration of the mechanical changes was consistent with a mechanical signal for compensatory growth.

Introduction

Post-pneumonectomy lung growth is a dramatic example of adult tissue morphogenesis. In many mammalian species, removal of one lung is associated with compensatory growth of

Correspondence: Dr. Steven J. Mentzer, Room 259, Brigham &Women's Hospital, 75 Francis Street, Boston, MA 02115 smentzer@partners.org.

Conflicts of Interest
None.

the remaining lung to near-baseline levels. The growth of the remaining lung reflects not simply an increase in alveolar size, but an increase in the number of alveoli [1]. The consequences of this process have been well-documented [2]; but the mechanisms controlling compensatory lung growth are unknown.

Although the potential importance of oxygen concentration [3], blood flow [4] and growth factors [5] to post-pneumonectomy growth have been reported, “alveolar-capillary stretch” [6] is generally considered the major factor controlling compensatory growth. The evidence for mechanical stretch is based on several indirect observations. Foremost, a reproducible experimental observation is that preventing stretch of the post-pneumonectomy lung by packing of the residual intrathoracic space with inert material limits compensatory growth [7-9]. Conversely, increasing the post-pneumonectomy stretch appears to increase compensatory growth. Maneuvers such as increasing the amount of lung resected (right lung versus left lung) [10], expanding the size of the chestwall with low atmospheric pressure [7] and in vitro overexpansion of the isolated perfused lung [11] produce responses consistent with enhanced growth. In addition, lung growth preferentially occurs in the cardiac lobe and in subpleural regions of the cardiac lobe—a spatial dependency consistent with stretch [12].

Recent studies of post-pneumonectomy lung cells [12], including endothelial cells [13, 14] and alveolar macrophages [15], have demonstrated an unexpected transcriptional time course; that is, gene transcription and cell proliferation that are minimal at 3 days, but peak 6 to 7 days after pneumonectomy. Distinct from the stretch responses studied in vitro—typically detected within hours of the stretch signal—these results indicate that post-pneumonectomy mechanics may not be optimally characterized as an immediate one-time stretch signal, but rather as dynamic anatomical and mechanical adaptations to the post-pneumonectomy thorax that occur over days to weeks.

The observations of post-pneumonectomy lung cell populations predict that relevant anatomic and mechanical changes occur within days of pneumonectomy—prior to the maximal transcriptional and proliferative response. To test this prediction, we investigated the anatomic changes and tissue mechanics during post-pneumonectomy lung growth by obtaining serial microCT scans and measuring respiratory system impedance. For mechanical forces to be causally implicated in compensatory lung growth, we anticipated that peripheral mechanical changes would be detectable prior to and resolve with compensatory growth.

Methods

Mice

8 to 12 week old C57/B6 mice (Jackson Laboratory, Bar Harbor, ME, USA), 22 to 30gm, were used in all experiments. The care of the animals was consistent with guidelines of the American Association for Accreditation of Laboratory Animal Care (Bethesda, MD, USA) with the protocol reviewed and approved by the Harvard Medical School Institutional Animal Care and Use Committee.

Anesthesia and intubation

The animals were anesthetized with an intraperitoneal injection of Ketamine 100 mg/kg (Fort Dodge Animal Health, Fort Dodge, IA, USA) and Xylazine 6 mg/kg (Phoenix Scientific, Inc., St. Joseph, MO). The animals were intubated under direct visualization with a standard 20g Angiocatheter (pneumonectomy) or 18g Angiocatheter (forced oscillation measurements)(BD Insyte, Sandy, UT, USA) using a thin metal stylus, and transferred to a FlexiVent rodent ventilator (SCIREQ, Montreal, QC Canada). Ventilator rates of 200/minute, tidal volume of 10 ml/kg with positive end-expiratory pressures of 3 cmH_2O and a pressure limit of 30 cmH_2O were used.

Pneumonectomy

In all mice, the left lung was exposed with a 5^{th} intercostal space thoracotomy and the hilum ligated with a 5-0 silk tie (Ethicon, Somerville, NJ, USA)[16]. The left lung was excised distal to the tie. For sham operated controls, the thoracotomy was created but the left lung left in situ. A recruitment maneuver (named “TLC” by SCIREQ), consisting of a 3 sec ramp to 30 cmH_2O follwed by a 3 sec hold, was performed while closing the thoracotomy. The animals were removed from the ventilator and extubated upon recovery of spontaneous respirations. The animals were recovered with supplemental oxygen and external warming; Subcutaneous Buprenorphine 2.4 μg (Hospira Inc., Lake Forest, IL, USA) was administered twice daily for 48 hours. There were no perioperative (post-pneumonectomy) deaths.

Pulmonary Mechanics

Prior to all measurements, the pressure transducers and ventilator tubing of the FlexiVent (SCIREQ) were calibrated by the two collected-point method. The volume and resistance of the endotracheal tube were calibrated with open and closed measurements. After intubation, mice were transferred to the FlexiVent system (SCIREQ) for pulmonary mechanics studies. Pulmonary mechanics on individual mice were measured immediately post-pneumonectomy and on days 3, 7, 14 and 21 post-procedure. The post-pneumonectomy mechanics were performed as a terminal procedure. The animals were hyperventilated at a rate of 300/minute and allowed to remove spontaneous respiratory drive and allowed to acclimate to the ventilator for two minutes before standardization of the volume history with 3 consecutive recruitment maneuvers (“TLC” by SCIREQ). Two maneuvers were performed. First, ventilation was briefly stopped and the animal passively exhaled to functional residual capacity (FRC); an 8 second multifrequency (0.5-19.5 Hz) oscillatory signal (Prime-8 by SCIREQ) was delivered with ventilation resumed at the completion of the maneuver. Second, dynamically determined pressure volume loops (PV-P by SCIREQ) were created by an 8-second steady inflation ramp to 30 cmH_2O, starting from a positive end-expiratory pressure (PEEP) of 3 cmH_2O, with an 8-second deflation. The PEEP of 3 cmH_2O was used to maintain lung volumes [16].

Input impedance model

Respiratory system impedance (Z_{rs}) includes the components representing the lung (Z_L) and chest wall (Z_w) [17]. Preliminary experiments demonstrated that the chest wall (Z_w) contributed less than 15% to absolute impedance measurements and did not influence the

time course or reproducibility of the observed mechanical changes in the lung. The constant phase model [18] was fitted to the input impedance to derive Newtonian resistance (R_n), tissue damping (G), tissue elastance (H) and hysteresivity (η) as described below:

$$Z_{rs} = R_n + j\omega I + (G - {}_iH) / \omega^{\alpha} \text{ where } \alpha = (2 / \pi)\tan^{-1}(1 / \eta) \text{ and } \eta = G / H$$

In this study, measurements were obtained at low frequencies and FRC; therefore, inertance (I) was negligible. A minimum of three measures were taken per animal with measurements accepted at a minimum coefficient of determination (COD) of 0.89; consistently high COD suggested input impedance with a high signal to noise ratio.

CT scanning

Prior to all imaging sessions, the CT scanner (GE explore VISTA, GE Healthcare, Waukesha, WI, USA) was set to a potential of 40kV and a current of 140uA. The animal was anesthetized in a chamber of 3% isofluorane and intubated with a 20g Angiocatheter. A volume controlled ventilator with the settings of 500ul tidal volume, 80/min respiratory rate and 0 PEEP was attached, and anesthesia maintained with 1.5% isofluorane. Cranial and caudal endpoints were defined, and the animal imaged at 4 shots per gantry turn at standard resolution (120um/slice). Upon completion of imaging, the animal was recovered in a warmed cage and studied on days 0, 3. 7, 14 and 21 post pneumonectomy.

Morphometry

The microCT images were archived as DICOM files and imported into MetaMorph 7.7 (Molecular Devices, Brandywine, PA, USA). After X, Y and Z axis distance calibration, the image planes were analyzed by MetaMorph to provide three-dimensional structural information. The *View Orthogonal Planes* command allowed examination of cross sectional slices through the image volume in the XY, XZ, and YZ planes [19]. The command permitted the use of sliders to select the X, Y, and Z coordinates of the active pixel location as it was displayed in each image window. The command was also used simultaneously with the *Measure XYZ Distance* command to draw wireframe lines to follow anatomic objects through multiple planes of the stack. The lines were viewed as an overlay on both the original stack and on the orthogonal plane stacks. XYZ coordinates were also exported for quantitative analysis.

Topographic mapping

After routine distance calibration, the microCT image stacks were separately processed for the heart, cardiac lobe, mediastinum and chestwall. For the heart, cardiac lobe and chestwall, axial microCT images at the T8-T9 intervertebral space were exported and recombined as a time series image stack in MetaMorph 7.7 (Molecular Devices). For the mediastinum, the image stack was processed using the MetaMorph *Stack Arithmetic Minimum* function. The stack minimum image, reflecting the carina and mainstem bronchi, was exported and recombined as a times series image stack. In each case, the region of interest was thresholded, binarized and the time series recombined using the *Topographic Surface* command.

Statistical analysis

Data analysis was performed using XLstat (Addinsoft, New York, NY, USA) add-in for Microsoft Excel. Results are reported as mean +/- one standard deviation (SD) unless otherwise noted. Statistical significance was determined using analysis of variance (ANOVA) with a p-value of 0.05. Pairwise comparisons were performed as needed using Tukey's test.

Results

Structural adaptations

To investigate the structural adaptations of the mouse thorax post-pneumonectomy, serial microCT imaging was performed (Figure 1). Analysis of the microCT scans demonstrated an ex vacuo pneumothorax detectable immediately post-operation (Figure 1B, arrow), but there was no residual air demonstrable by post-operative day 3. Morphometry of the cardiac silhouette demonstrated initial cardiac enlargement (axis length 8.1±0.3mm day 0 versus 7.3±0.2mm control), then shift of the heart into the left hemithorax (Figure 2A). The most striking change in pulmonary anatomy was a shift of the cardiac lobe into the left hemithorax; mean displacement of the lobar centroid was 5.2±0.8mm (Figure 2B). In contrast, there was minimal displacement of the trachea or carina (range 0-3 mm) at any point post-operation (Figure 2C). Similarly, the postoperative chestwall configuration was similar to the control mice with no consistent asymmetries (Figure 2D).

Lung volume changes

Based on microCT images, volumetric reconstructions demonstrated an initial decline in total lung volumes followed by progressive enlargement of the remaining lung (Figure 3A). Comparison of the no surgery age-matched controls and post-pneumonectomy day 21 mice demonstrated no significant difference in total lung volumes (Figure 3B; $p>.05$). To determine the coincident mechanical changes, the pressure (P)-volume (V) relationship of the post-pneumonectomy lung was studied. Quasi-static deflation lung P-V curves demonstrated a comparable shape at 4 time points after pneumonectomy (Figure 3C). Additionally, the volume of the compensatory lung on day 21 was not statistically different from the control volume of control lungs at 30 cmH_2O distending pressure (Figure 3D). Despite the similarity of the P-V curves, measures of quasi-static compliance (decreased) and elastance (increased) were significantly changed at all time points post-pneumonectomy ($p < 0.01$)(Figure 4A). These measures peaked on day 3 (0.065 cmH_2O/ml and 15.33 ml/cmH_2O). Lung distensibility, a reflection of specific compliance, peaked on day 3 and normalized to prepneumonectomy levels by day 7 (Figure 4B).

Pressure-flow response

To identify a characteristic frequency dependence produced by parenchymal lung growth, the lungs of post-pneumonectomy mice were probed using the forced oscillation technique. At frequencies below 5 Hz, a significant difference in the flow resistive properties of the respiratory system was noted on day 3 after pneumonectomy ($p<.05$); no difference was identified between control and pneumonectomy mice at other time points (Figure 5). At

frequencies above 5 Hz, there was no significant difference between pneumonectomy and control mice at any time point.

Constant-phase model

Fitting the constant phase model to respiratory system impedance data produced measures of Newtonian resistance (R_n), tissue damping (G), elastance (H), and hysteresivity (η)(Figure 6). Newtonian resistance peaked immediately post-procedure (0.35 $cmH_2O.s/ml$) and rapidly returned to baseline levels by day 3 after pneumonectomy (0.25 $cmH_2O.s/ml$). Tissue damping and elastance remained elevated on day 3 (5.8 and 32.7 cmH_2O/ml), and returned to baseline by day 7 (4.5 and 27.9 cmH_2O/ml, $p < 0.05$). Hysteresivity was unchanged at all time points (mean = 0.17). For all parameters, there was no significant difference between no surgery mice and sham thoracotomy controls ($p > .05$; N=4; day 3).

Discussion

In this report, we investigated the mechanostructural changes during murine post-pneumonectomy lung growth. Our studies demonstrated 1) significant displacement of the heart and cardiac lobe within 3 days of surgery, and 2) coincident changes in peripheral lung mechanics. The changes in both the anatomic configuration of the thorax and the impedance measurements within the lung preceded the previously described peaks in growth-associated gene transcription [13, 15]. Further, the peripheral mechanical changes in the lung resolved with compensatory growth. We conclude that the timing and duration of the mechanical changes was consistent with a mechanical signal for compensatory growth.

The gross anatomic changes after left pneumonectomy provided insight into the structural mechanics of the mouse thorax. In the normal mouse, the reproducibility of thoracic anatomy indicates a mechanostructural equilibrium. The significant displacement of the heart and cardiac lobe within days of surgery suggests that this stable structural system was destabilized by pneumonectomy. A new structural equilibrium was subsequently established after anatomic realignment. Of note, the cardiac lobe was the portion of the lung with the greatest displacement; it is also the lobe of the lung with the greatest demonstrable post-pneumonectomy increase in angiogenesis [12], volume [4, 20-22], weight [23] and cell proliferative activity [21, 24, 25]. Since structural hierarchies channel mechanical forces from the macroscale to microscale, it is likely that the post-pneumonectomy mechanical instabilities were transmitted down to the level of lung cells. Work in cellular signal transduction suggests that these mechanical signals may contribute to the trigger for cellular proliferation and tissue remodeling [26].

The impact of pneumonectomy was reflected in our measurements of lung tissue impedance; namely, our measurements of tissue damping (G) and elastance (H). A measure of the in-phase pressure losses across the lung tissue, tissue resistance has been thought to reflect frictional losses occurring at an elemental level; that is, at a level coupling energy dissipation and elastic behavior [27]. The mechanism responsible for this structural damping is unclear, but likely reflects components intimately involved in tissue regeneration including proliferating cells, extracellular connective tissue and the alveolar air-liquid interface [28, 29]. Consistent with this interpretation, our data demonstrated a significant

change in tissue damping coincident with the maximal growth phase; that is, the phase of lung growth associated with cellular proliferation and gene transcription [12-14]. We speculate that the return to baseline G and H was a reflection of neoalveolarization.

The interpretation that changes in tissue impedance may reflect neoalveolarization is also supported by observations in developing rat lungs. Respiratory mechanics in neonatal rats have demonstrated a significant decrease in tissue damping and elastance from postnatal days 10 to 16. These changes temporally coincide with alveolarization and the thinning of alveolar septae [30]. Similarly, an association of tissue resistance with alveolar wall thickness is consistent with observations in pathologic conditions [31, 32]. Finally, a prediction based on the dominance of damping and elastance measures at TLC is that tissue damping (G) should increase if volume changes were due to alveolar hyperinflation without tissue growth [33]; the observed decrease in tissue damping is further mechanical evidence for lung growth.

Previous attempts to characterize the anatomy and respiratory mechanics after pneumonectomy in animal models have focused on the functional consequences of compensatory growth. Consistent with our findings, previous studies have demonstrated that anatomic volume of the remaining lung at the completion of compensatory growth approximated baseline lung volumes [2]. Also consistent with the present work, studies of mechanical deformation of the lung during inspiration and expiration have approximated normal. For example, pressure-volume curves appeared normal when volume was expressed as a percentage of maximal lung volumes [34, 35]. Despite the normal shape of the flow-volume curve and retained elastic recoil, the lung volume at any given distending pressures is consistently lower in pneumonectomized rats than in the two lungs of control rats [34, 35]. Perhaps reflecting a growth-related change in the conducting airways, decreased maximal expiratory flow rates have been noted post-pneumonectomy [36-39]. The reduced maximal flow rates appear to be related to both increased upstream resistance and abnormal central airway mechanics [39].

Despite the detectable mechanical changes in the remaining lung after left pneumonectomy, our study has a number of limitations. From a methodologic viewpoint, our studies were performed with the chest wall intact. Although we used hyperventilation and sedation to minimize the contribution of the chest wall, the potential contribution of the chest wall will need to be studied in future work. Similarly, the use of plastic (not metal) cannulae and a single level of PEEP (3 cmH2O) are methodologic choices that may benefit from separate study. From a biologic viewpoint, our manipulation was limited to left pneumonectomy. We did not separately manipulate the potential components of lung impedance; namely, the amount of lung tissue and pulmonary blood flow. Based on this study and prior work [40], we anticipate that lung volume and blood volume will have reciprocal influences on tissue resistance.

Finally, an intriguing observation was the relative stability of hysteresivity (η) during the process of presumed neoalveolarization. Hysteresivity, an empirically determined variable that quantifies the dependence of energy dissipative processes on elastic processes, would reasonably change with the changing composition of the peripheral lung. Cell proliferation

and extracellular matrix biosynthesis would likely change this energy relationship. Similarly, the development of alveolar form—the spatial relationship of these materials—would likely change the mechanical interaction among those materials. Despite these predictions, the relationship of energy dissipation to energy storage as measured by η did not change during the compensatory growth phase. An interesting possibility is that tissue growth proceeds with hysteretic matching; that is, the rate and locality of cell proliferation and matrix production is tied to the elastic actions of a particular region of the lung. This possibility suggests a mechanistic link, perhaps reflecting feedback control, between the trigger for and the consequences of lung growth.

Acknowledgments

We acknowledge Mi-Ae Park and Shuyan Wang for their assistance with microCT imaging.

This work was supported in part by NIH Grant HL94567, HL75426, and HL007734 as well as the Uehara Memorial Foundation and the JSPS Postdoctoral Fellowships for Research Abroad.

Abbreviations

FRC	functional residual capacity
G	tissue damping
H	tissue elastance
I	inertance
IP	intraperitoneal
MLI	mean linear intercept
PEEP	positive end-expiratory pressures
P	pressure
Rn	Newtonian resistance
RM	recruitment maneuver
SA	surface area
SD	standard deviation
V	volume

References

1. Fehrenbach H, Voswinickel R, Michl V, Mehling T, Fehrenbach A, Seeger W, Nyengaard JR. Neoalveolarisation contributes to compensatory lung growth following pneumonectomy in mice. Eur. Respir. J. 2008; 31:515–522. [PubMed: 18032439]
2. Hsia CCW, Berberich MA, Driscoll B, Laubach VE, Lillehei CW, Massaro C, Perkett EA, Pierce RA, Rannels DE, Ryan RM, Tepper RS, Townsley MI, Veness-Meehan KA, Wang N, Warburton D. Mechanisms and limits of induced postnatal lung growth. Am. J. Respir. Crit. Care. Med. 2004; 170:319–343. [PubMed: 15280177]
3. Sekhon HS, Smith C, Thurlbeck WM. Effect of hypoxia and hyperoxia on postpneumonectomy compensatory lung growth. Exp. Lung Res. 1993; 19:519–532. [PubMed: 8253056]

4. Fernandez LG, Le Cras TD, Ruiz M, Glover DK, Kron IL, Laubach VE. Differential vascular growth in postpneumonectomy compensatory lung growth. J. Thorac. Cardiovasc. Surg. 2007; 133:309–316. [PubMed: 17258553]
5. McAnulty RJ, Guerreiro D, Cambrey AD, Laurent GJ. Growth factor activity in the lung during compensatory growth after pneumonectomy - evidence of a role for IGF-1. Eur. Respir. J. 1992; 5:739–747. [PubMed: 1628732]
6. Hsia CCW, Herazo LF, Fryderdoffey F, Weibel ER. Compensatory lung growth occurs in adult dogs after right pneumonectomy. J. Clin. Invest. 1994; 94:405–412. [PubMed: 8040282]
7. Cohn R. Factors affecting the postnatal growth of the lung. Anat. Rec. 1939; 75:195–205.
8. Fisher JM, Simnett JD. Morphogenetic and proliferative changes in regenerating lung of rat. Anat. Rec. 1973; 176:389–395. [PubMed: 4723402]
9. Brody JS, Burki R, Kaplan N. Deoxyribonucleic-acid synthesis in lung-cells during compensatory lung growth after pneumonectomy. Am. Rev. Respir. Dis. 1978; 117:307–316. [PubMed: 637412]
10. Hsia CCW, Fryderdoffey F, Staldernavarro V, Johnson RL, Reynolds RC, Weibel ER. Structural changes underlying compensatory increase of diffusing capacity after left pneumonectomy in adult dogs. J. Clin. Invest. 1993; 92:758–764. [PubMed: 8349815]
11. Russo LA, Rannels SR, Laslow KS, Rannels DE. Stretch-related changes in lung cAMP after partial pneumonectomy. Am. J. Physiol. 1989; 257:E261–E268. [PubMed: 2548393]
12. Konerding MA, Gibney BC, Houdek J, Chamoto K, Ackermann M, Lee G, Lin M, Tsuda A, Mentzer SJ. Spatial dependence of alveolar angiogenesis in post-pneumonectomy lung growth. Angiogenesis. 2012; 15:23–32. [PubMed: 21969134]
13. Lin M, Chamoto K, Gibney B, Lee GS, Collings-Simpson D, Houdek J, Konerding MA, Tsuda A, Mentzer SJ. Angiogenesis gene expression in murine endothelial cells during post-pneumonectomy lung growth. Resp. Res. 2011; 12:98.
14. Chamoto K, Gibney BC, Lee GS, Lin M, Simpson DC, Voswinckel R, Konerding MA, Tsuda A, Mentzer SJ. CD34+ progenitor to endothelial cell transition in post-pneumonectomy angiogenesis. Am. J. Resp. Cell Mol. Biol. 2012 In press.
15. Chamoto K, Gibney BC, Ackermann M, Lee GS, Lin M, Konerding MA, Tsuda A, Mentzer SJ. Alveolar macrophage dynamics in murine lung regeneration. J. Cell. Physiol. 2012 In press.
16. Gibney B, Lee GS, Houdek J, Lin M, Chamoto K, Konerding MA, Tsuda A, Mentzer SJ. Dynamic determination of oxygenation and lung compliance in murine pneumonectomy. Exp. Lung Res. 2011; 37:301–309. [PubMed: 21574875]
17. Hantos Z, Adamicza A, Govaerts E, Daroczy B. Mechanical impedances of lungs and chest-wall in the cat. J. Appl. Physiol. 1992; 73:427–433. [PubMed: 1399961]
18. Hantos Z, Daroczy B, Suki B, Nagy S, Fredberg JJ. Input impedance and peripheral inhomogeneity of dog lungs. J. Appl. Physiol. 1992; 72:168–178. [PubMed: 1537711]
19. Ravnic DJ, Tsuda A, Turhan A, Zhang Y-Z, Pratt JP, Huss HT, Mentzer SJ. Multi-frame particle tracking in intravital imaging: defining lagrangian coordinates in the microcirculation. BioTechniques. 2006; 41:597–601. [PubMed: 17140117]
20. Rannels DE, Stockstill B, Mercer RR, Crapo JD. Cellular-changes in the lungs of adrenalectomized rats following left pneumonectomy. Am. J. Respir. Cell Mol. Biol. 1991; 5:351–362. [PubMed: 1910820]
21. Voswinckel R, Motejl V, Fehrenbach A, Wegmann M, Mehling T, Fehrenbach H, Seeger W. Characterisation of post-pneumonectomy lung growth in adult mice. Eur. Respir. J. 2004; 24:524–532. [PubMed: 15459128]
22. Sekhon HS, Thurlbeck WM. A comparative-study of postpneumonectomy compensatory lung response in growing male and female rats. J. Appl. Physiol. 1992; 73:446–451. [PubMed: 1399964]
23. Rannels DE, White DM, Watkins CA. Rapidity of compensatory lung growth following pneumonectomy in adult rats. J. Appl. Physiol. 1979; 46:326–333. [PubMed: 422449]
24. Cagle PT, Langston C, Goodman JC, Thurlbeck WM. Autoradiographic assessment of the sequence of cellular proliferation in postpneumonectomy lung growth. Am. J. Respir. Cell Mol. Biol. 1990; 3:153–158. [PubMed: 2378749]

25. Thet LA, Law DJ. Changes in cell number and lung morphology during early postpneumonectomy lung growth. J. Appl. Physiol. 1984; 56:975–978. [PubMed: 6725076]
26. Tschumperlin DJ, Boudreault F, Liu F. Recent advances and new opportunities in lung mechanobiology. J. Biomech. 2010; 43:99–107. [PubMed: 19804885]
27. Fredberg JJ, Stamenovic D. On the imperfect elasticity of lung tissue. J. Appl. Physiol. 1989; 67:2408–2419. [PubMed: 2606848]
28. Mijailovich SM, Stamenovic D, Fredberg JJ. Toward a kinetic theory of connective tisue micromechanics. J. Appl. Physiol. 1993; 74:665–681. [PubMed: 8458781]
29. Faffe DS, Zin WA. Lung parenchymal mechanics in health and disease. Physiol. Rev. 2009; 89:759–775. [PubMed: 19584312]
30. Burri PH, Dbaly J, Weibel ER. Postnatal-growth of rat lung.1. Morphometry. Anat. Rec. 1974; 178:711–730.
31. Dolhnikoff M, Mauad T, Ludwig MS. Extracellular matrix and oscillatory mechanics of rat lung parenchyma in bleomycin-induced fibrosis. Am. J. Respir. Crit. Care. Med. 1999; 160:1750–1757. [PubMed: 10556151]
32. Pillow JJ, Hall GL, Willet KE, Jobe AH, Hantos Z, Sly PD. Effects of gestation and antenatal steroid on airway and tissue mechanics in newborn lambs. Am. J. Respir. Crit. Care. Med. 2001; 163:1158–1163. [PubMed: 11316653]
33. Thamrin C, Janosi TZ, Collins RA, Sly PD, Hantos Z. Sensitivity analysis of respiratory parameter estimates in the constant-phase model. Ann. Biomed. Eng. 2004; 32:815–822. [PubMed: 15255212]
34. Buhain WJ, Brody JS. Compensatory growth of lung following pneumonectomy. J. Appl. Physiol. 1973; 35:898–902. [PubMed: 4765830]
35. Bennett RA, Addison JL, Rannels DE. Static mechanical-properties of lungs from adrenalectomized pneumonectomized rats. Am. J. Physiol. Heart Circ. Physiol. 1987; 253:E6–E11.
36. Yee NM, Hyatt RE. Effect of left pneumonectomy on lung-mechanics in rabbits. J. Appl. Physiol. 1983; 54:1612–1617. [PubMed: 6874484]
37. Greville HW, Arnup ME, Mink SN, Oppenheimer L, Anthonisen NR. Mechanism of reduced maximum expiratory flow in dogs with compensatory lung growth. J. Appl. Physiol. 1986; 60:441–448. [PubMed: 3949649]
38. Mink SN, Holtby SG, Berezanski DJ, Oppenheimer L, Anthonisen NR. Heterogeneity of maximal lobar emptying rates in dogs with compensatory lung growth. J. Appl. Physiol. 1989; 67:1164–1170. [PubMed: 2793708]
39. Georgopoulos D, Mink SN, Oppenheimer L, Anthonisen NR. How is maximal expiratory flow reduced in canine postpneumonectomy lung growth. J. Appl. Physiol. 1991; 71:834–840. [PubMed: 1757319]
40. Giannell S, Ayres SM, Buehler ME. Effect of pulmonary blood flow upon lung mechanics. J. Clin. Invest. 1967; 46:1625–1642. [PubMed: 6061740]

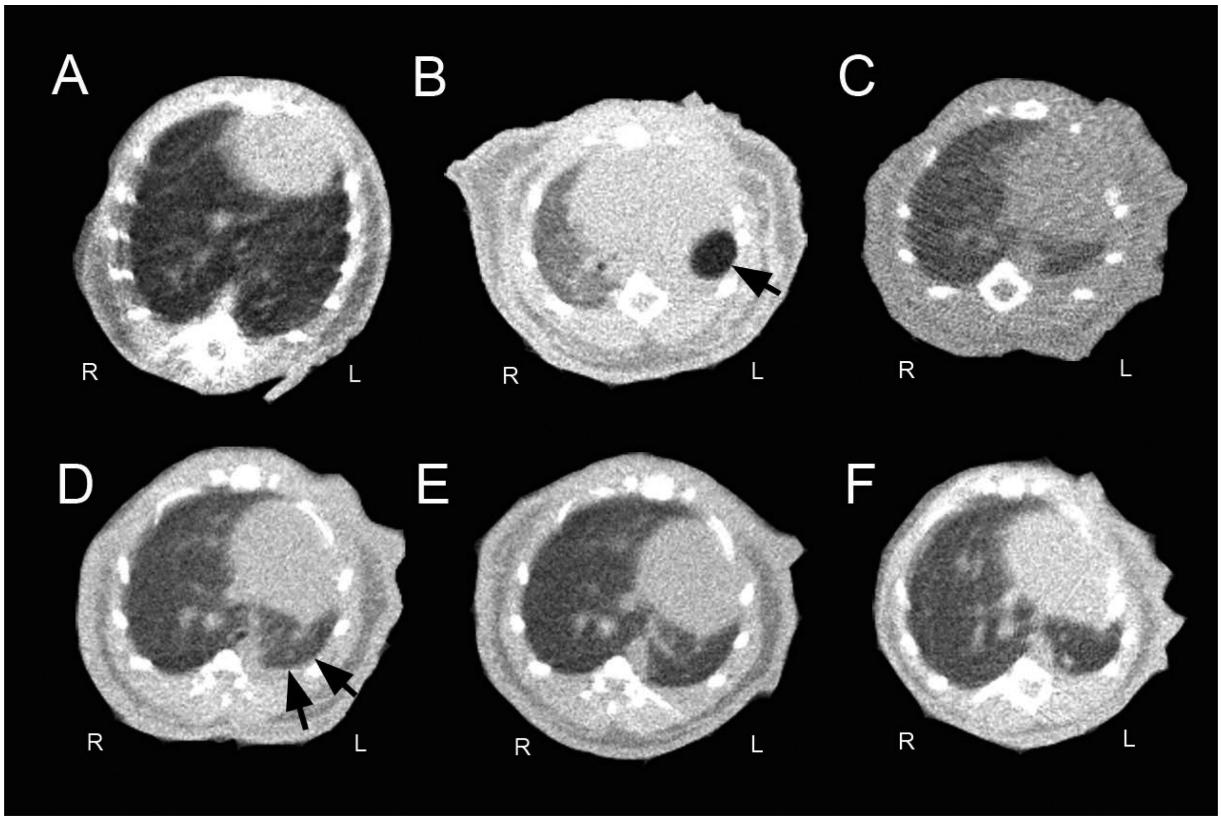

Figure 1.

Thorax anatomy after left pneumonectomy. Representative microCT scans obtained pre-pneumonectomy (A) as well as 3 hours (B), 3 days (C), 7 days (D), 14 days (E) and 21 days (F) post-pneumonectomy (B), The transverse axial images were obtained at the level of the T9 vertebral body. The post-pneumonectomy space (single arrow) was replaced by the cardiac lobe (double arrow).

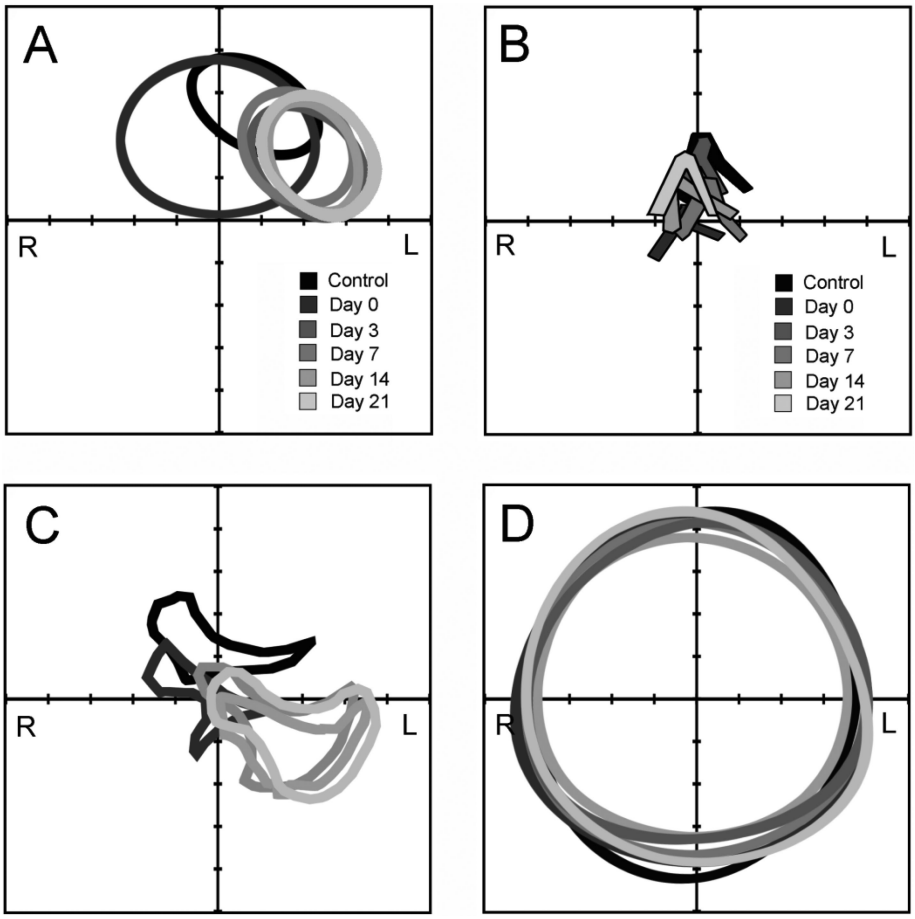

Figure 2.

Anatomic changes in the murine thorax after left pneumonectomy. Transverse axial microCT images analyzed on nonsurgical age-matched mice (Control), 3 hours after surgery (Day 0), and on days 3, 7, 14, and 21 days after left pneumonectomy. XY axis was oriented on the anatomic centroid of the animal in the transverse plane. A) Cardiac silhouette measured at T9 was thresholded and perimeter outlined; the enlarged silhouette reflects Day 0 (arrow). B) Mediastinum was assessed by mainstem bronchial airway orientation in the transverse plane. The cross-section of the cardiac lobe was outlined at the level of the T8-T9 vertebral body. D) The chest wall contour was thresholded at the level of the T8-T9 vertebral body. Representative CT scans of 3-4 mice at each time point are shown.

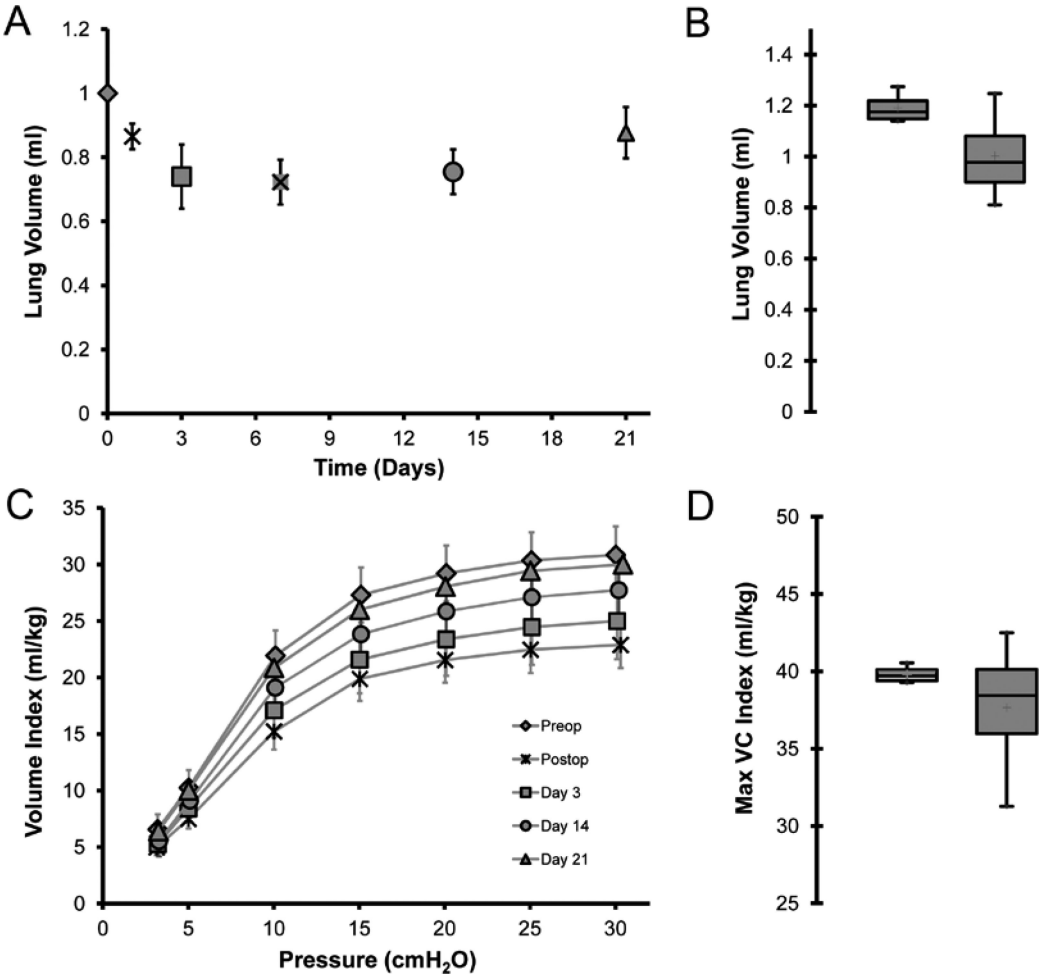

Figure 3.

Lung volumes after pneumonectomy. A) Lung volumes calculated using 3D reconstructions of microCT images (120um/pixel resolution) with volume averaging over 120um intervals. The images were obtained with positive pressure ventilation at 14ul/gm (N=3-4 mice per data point). B) Comparison of lung volumes of control mice (2 lungs, left) and post-pneumonectomy day 21 mice (1 lung, right)(N=3-4 mice per data point). C) Quasi-static deflation limbs of the pressure volume loop post-pneumonectomy; lung volumes were normalized to mouse body weight (Volume Index). Lung volumes were compared prior to surgery (Control), immediately after surgery (Day 0)(N=8), as well as on days 3, 7, 14, and 21 after pneumonectomy (N=8-14 at each time point). D) Comparison of lung volumes of control mice (2 lungs, left) and post-pneumonectomy day 21 mice (1 lung, right). Values reflect FlexiVent delivered volumes at 30cmH_2O distending pressure normalized to body weight (Maximum Vital Capacity Index). The data was plotted with the box defining the 25th and 75th percentiles with the whiskers defining the 5th and 95th percentile. The median value was plotted as a red cross (p=0.39).

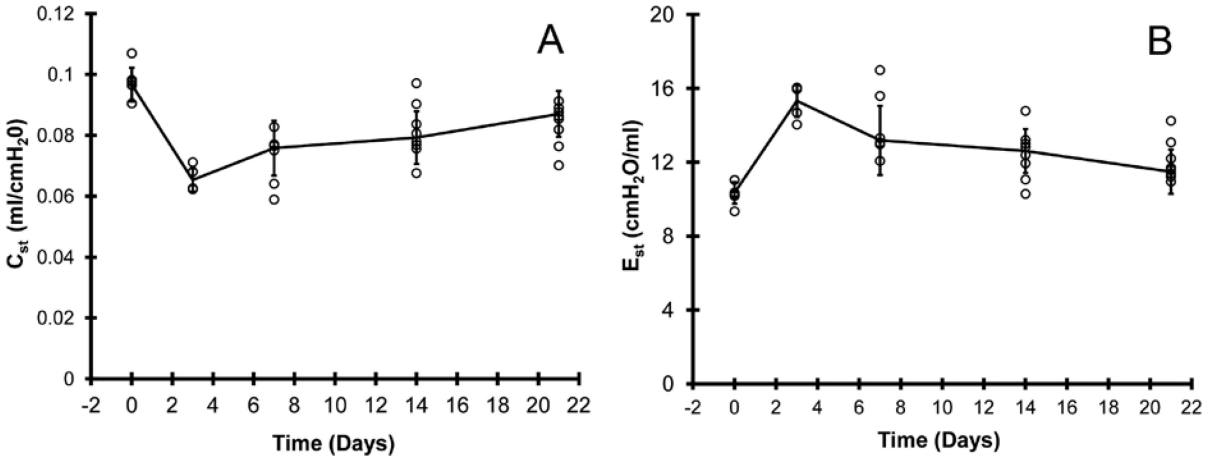

Figure 4.

The shapes of the pressure volume loops were used to derive A) quasi-static compliance (Cst), and B) quasi-static elastance (Est) data. Each data point reflects the mean volume of one mouse; error bars reflect 1 SD.

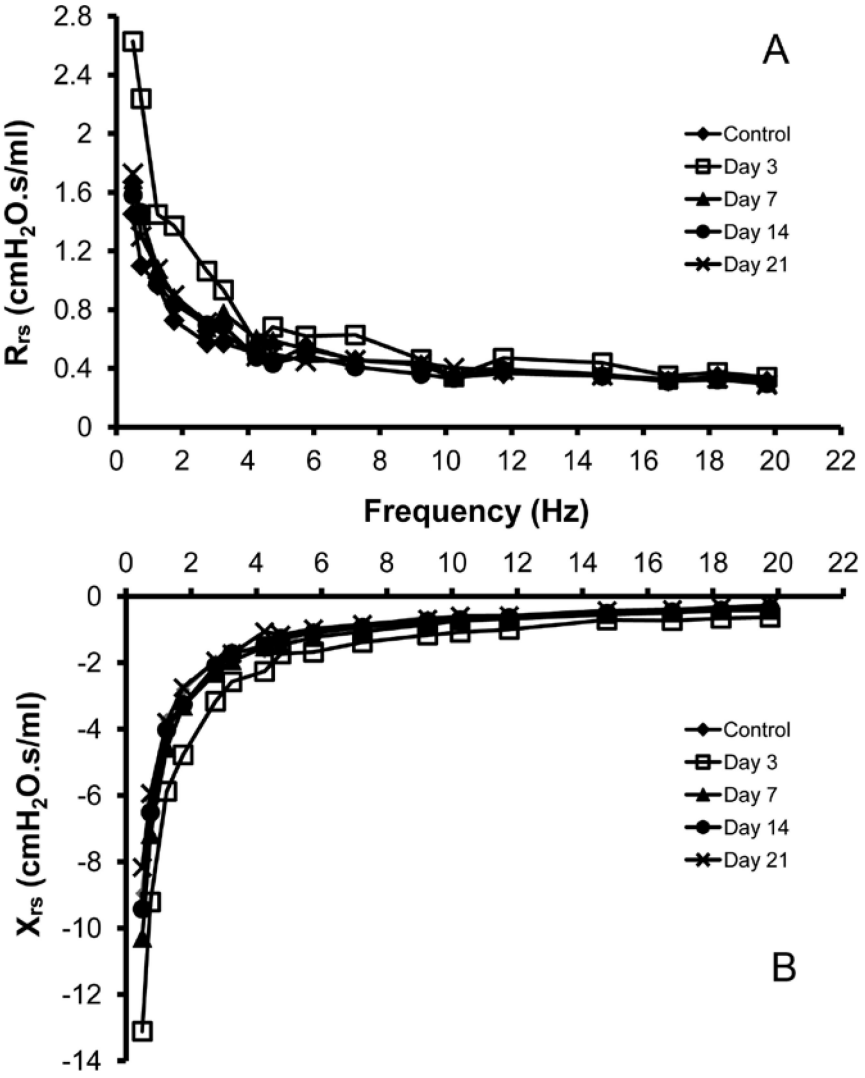

Figure 5.

Impedance measurements of the respiratory system. Forced oscillation measurements were obtained in control mice and 3, 7, 14 and 21 days post-pneumonectomy. Total respiratory system resistance (R_{rs})(A, real part) and reactance (X_{rs})(B, imaginary part) are displayed in the frequency domain. Representative values are shown.